# Role of Lone-Pair Electrons in Producing Minimum Thermal Conductivity in Nitrogen-Group Chalcogenide Compounds

Eric J. Skoug* and Donald T. Morelli

*Department of Chemical Engineering and Materials Science Michigan State University East Lansing, Michigan, 48824, USA*

(Received 29 August 2011; published 30 November 2011)

Fully dense crystalline solids with extremely low lattice thermal conductivity ($\kappa_L$) are of practical importance for applications including thermoelectric energy conversion and thermal barrier coatings. Here we show that lone-pair electrons can give rise to minimum $\kappa_L$ in chalcogenide compounds that contain a nominally trivalent group VA element. Electrostatic repulsion between the lone-pair electrons and neighboring chalcogen ions creates anharmonicity in the lattice, the strength of which is determined by the morphology of the lone-pair orbital and the coordination number of the group VA atom.

DOI: 10.1103/PhysRevLett.107.235901 PACS numbers: 65.40.−b, 61.50.−f, 66.70.−f

The transport of heat in crystalline solids has long been a topic of interest in solid-state physics. Debye first studied heat transport by lattice phonons in 1912 [1] and to this day the lattice thermal conductivity ($\kappa_L$) of a vast array of crystalline materials can be estimated, to a first approximation, using some form of the Debye model. An interesting problem arises when one encounters a material whose lattice thermal conductivity cannot be explained using conventional phonon transport theory, as in the case of an ordered crystal that exhibits "minimum thermal conductivity" ($\kappa_{\rm min}$) behavior at ordinary temperatures. Slack first introduced this concept, which he defined as the case where all phonons are scattered so frequently that the average mean free path is on the order of 1 phonon wavelength [2]. It is not uncommon for $\kappa_L$ of an ordered crystal to approach $\kappa_{\rm min}$ near its melting temperature due to intrinsic phonon-phonon interactions alone; however similar behavior near room temperature is quite rare and the phonon scattering mechanisms that govern such behavior are not well understood. Here we show that lone electron pairs (LEPs) can produce $\kappa_{\rm min}$ behavior in group VA chalcogenides. Our results indicate that the morphology of the LEP is directly related to lattice anharmonicity, and the propensity of a given crystal to exhibit $\kappa_{\rm min}$ behavior can be predicted based on the local atomic environment of the group VA atom. A better understanding of intrinsically limited $\kappa_L$ is important to not only our fundamental picture of phonon transport in solids, but also has major implications in the design of high performance thermoelectric materials and thermal barrier coatings, which require materials with extremely low $\kappa_{\rm L}$.

We have recently shown that the compounds $\rm Cu_3SbSe_4$ and $\rm Cu_3SbSe_3$ possess vastly different $\kappa_L$ despite their similarities in average atomic mass and stoichiometry [3]. In the former compound, $\kappa_L$ increases rapidly with decreasing temperature due to vanishing phonon-phonon interactions (typical for a crystalline material), while the latter compound has a temperature independent $\kappa_L$ near its minimum possible value even at cryogenic temperatures. A similar situation occurs in the case of $\rm AgInTe_2$ versus $\rm AgSbTe_2$, where the $\kappa_L$ of the former compound is "normal" and the latter is glasslike [4,5]. The common thread among the compounds with anomalously low $\kappa_L$ is that they contain Sb nominally in the trivalent (+3) valence state, meaning that the Sb 5*s* electrons are nonbonding. Petrov and Shtrum originally proposed the idea that the "lone-pair" 5*s* electrons could interact with the valence electrons of adjacent atoms upon thermal agitation and cause increased anharmonicity in the lattice (thus lowering $\kappa_L$) [4], a concept recently revisited by Morelli *et. al.* [5]. This provides a qualitative explanation for the low intrinsic $\kappa_L$ of these compounds, but to our knowledge no direct evidence of a relationship between LEPs and low $\kappa_L$ has been presented.

The Cu-Sb-Se ternary system presents a unique opportunity to study the effect of LEPs on $\kappa_L$. In addition to $\rm Cu_3SbSe_4$ and $\rm Cu_3SbSe_3$, the compound $\rm CuSbSe_2$ forms readily and has a structure similar to that of $\rm Cu_3SbSe_3$ (orthorhombic, space group *Pmna* [6]). Naively one would expect these three compounds to all have $\kappa_L$ similar to that of $\rm Cu_3SbSe_4$ since their average atomic masses are nearly the same and none of them possesses an overly complex crystal structure. The only reasonable explanation for the large $\kappa_L$ discrepancy (see Fig. 1) is that there must be an intrinsic phonon scattering mechanism acting with increasing strength as the composition changes from $\rm Cu_3SbSe_4$ to $\rm CuSbSe_2$ to $\rm Cu_3SbSe_3$. These results are consistent with the hypothesis that the Sb 5*s* LEP gives rise to anharmonic forces in the lattice, but since Sb is nominally in the +3 state in both $\rm CuSbSe_2$ and $\rm Cu_3SbSe_3$ the $\kappa_L$ difference between these two compounds is not immediately clear.

In $\rm Cu_3SbSe_4$, Sb is coordinated by 4 selenium atoms with ideal tetrahedral Se-Sb-Se bond angles of 109.5° [7], suggesting $sp^3$ hybridization of the Sb valence electron orbitals. In this case, all of the Sb valence electrons form bonds with neighboring Se atoms. In $\rm CuSbSe_2$, however, Sb is coordinated by 3 Se atoms in a trigonal pyramidal configuration with an average Se-Sb-Se bond angle of

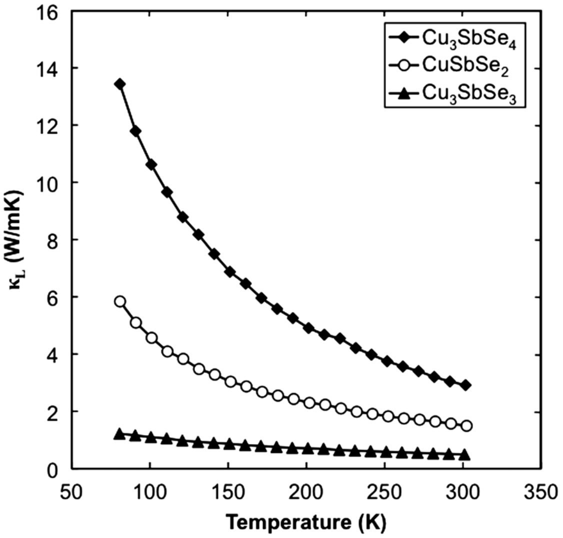

FIG. 1. Temperature dependence of the lattice thermal conductivity ($\kappa_L$) of $Cu_3SbSe_4$, $Cu_3SbSe_3$, and $CuSbSe_2$.

95.24° [6]. In this arrangement only the Sb $5p$ electrons form bonds with Se, leaving the Sb $5s$ electrons "free" to orient along the missing vertex of the tetrahedron, as defined by the valence shell electron pair repulsion theory. The configuration is similar for $Cu_3SbSe_3$ except the average Se-Sb-Se bond angle is 99.42°, intermediate to those of the other two compounds [8]. Once again the Sb $5s$ LEP forms an imperfect tetrahedron with the Sb $5p$ bonding electrons (see Fig. 2).

The coordination environment of Sb in $Cu_3SbSe_4$ requires little interpretation as it is analogous to the well-known group IV, III-V, and II-VI semiconductors. In $CuSbSe_2$ and $Cu_3SbSe_3$, however, Sb has the same coordination yet the average Se-Sb-Se angle is quite different. Wang and Liebau studied this effect, and found that the change in $X$-Sb-$X$ bond angle (where $X$ denotes a chalcogen atom) correlates to the stereochemical activity of the LEP, or the delocalization of the Sb $5s$ LEP away from the Sb nucleus [9]. This phenomenon stems from the fact that the actual valence of Sb in a given compound is not necessarily purely trivalent or pentavalent, but rather a combination of these two extremes. For a purely pentavalent Sb compound, as in the case of $Cu_3SbSe_4$, all of the Sb valence electrons are completely delocalized from the Sb nucleus and form bonds that assume the ideal tetrahedral angle of 109.5°. For a purely trivalent compound the Sb $5s$ electrons remain concentrated around the Sb nucleus, thereby inducing a Coulombic repulsion with the bonding Sb $5p$ electrons, causing the $X$-Sb-$X$ bond angle to decrease. As the actual Sb valence varies from +3 to +5 the $5s$ LEP progressively retracts from the nucleus, weakening the repulsion and causing the bond angle to increase. Wang and Liebau compiled average $X$-Sb-$X$ bond angles ($\bar{\alpha}$) from the literature and derived an expression for the effective valence of $Sb^{3+}$ in the $SbX_n$ polyhedral [9]:

$$^{\mathrm{eff}}V_{\mathrm{Sb}^{3+}}(\bar{\alpha}) = 3[1 + 0.0128(\bar{\alpha} - 90)]. \qquad (1)$$

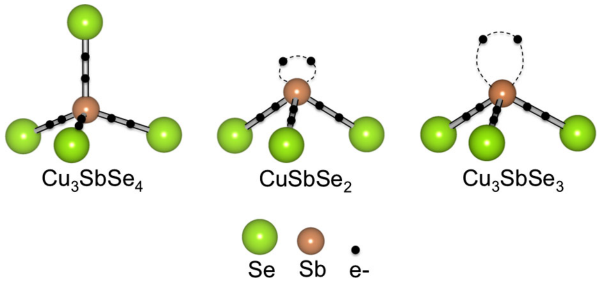

FIG. 2 (color online). Schematic representation of the local atomic environment of Sb in $Cu_3SbSe_4$, $Cu_3SbSe_3$, and $CuSbSe_2$. Shaded lines represent Sb-Se bonds, dashed lines illustrate the approximate morphology of the Sb lone-pair $5s$ electron orbital.

The difference in the Se-Sb-Se bond angle between $CuSbSe_2$ and $Cu_3SbSe_3$ can now be interpreted as a difference in effective Sb valence state. $^{\mathrm{eff}}V_{\mathrm{Sb}^{3+}} = 3.2$ for $CuSbSe_2$ and 3.36 for $Cu_3SbSe_3$, indicating that the LEP is farther removed from the Sb nucleus in the latter compound. The main idea behind the relationship between LEPs and low $\kappa_L$ is that as atoms approach one another during thermal agitation, the overlapping wave functions of the LEP and nearby valence electrons will induce a nonlinear repulsive electrostatic force causing increased anharmonicity in the lattice. As the LEP moves away from the Sb nucleus, anharmonic interactions with adjacent atoms intensify and $\kappa_L$ decreases. The highest degree of anharmonicity should thus be achieved when the LEP is far removed from the Sb nucleus yet not participating in bonding, intermediate to the case of $Sb^{3+}(\bar{\alpha} \approx 90°)$ and $Sb^{5+}$ ($\bar{\alpha} = 109.5°$). This explains the $\kappa_L$ difference between the three Cu-Sb-Se compounds shown in Fig. 1 and provides direct evidence in favor of a relationship between LEPs and $\kappa_L$. The acoustic mode Grüneisen parameters of $Cu_3SbSe_3$ and $Cu_3SbSe_4$, which quantify lattice anharmonicity in these compounds, have been obtained from density functional theory calculations and are in good agreement with these results (details to follow in a forthcoming publication [10]).

If there exists a universal relationship between LEP morphology and $\kappa_L$, then it should be possible to generalize the results of the Cu-Sb-Se compounds to other group VA chalcogenides. With this in mind, a comprehensive literature review of the crystal structures and room temperature $\kappa_L$ values of group VA chalcogenides was conducted. Literature data are given in Table I for compounds of the form $M_2X_3$ and $A_iM_jX_k$ where $M$ = As, Sb, or Bi, $X$ = S, Se, or Te, and $A$ = Cu, Ag, Tl, or an alkali metal. The average $X$-$M$-$X$ bond angles were calculated from the bond angles of the nearest neighbor $M$-$X$ bonds, which form the coordination polyhedra around the $M$ atoms.

TABLE I. Literature data for each compound plotted in Figs. 3 and 4.

| Compound | Crystal Structure (Space Group) | CN | $\bar{\alpha}$ (°) | $\kappa_L$ at 300 K | References [$\bar{\alpha}$], [$\kappa_L$] |
|---|---|---|---|---|---|
| $Sb_2S_3$ | Orthorhombic ($Pnma$) | 7 | 89.22 | 1.3 | [12], [13] |
| $Sb_2Se_3$ | Orthorhombic ($Pbnm$) | 7 | 90.00 | 1.0 | [9], [13] |
| $Sb_2Te_3$ | Rhombohedral ($R\bar{3}m$) | 6 | 88.00 | 2.4 | [14], [13] |
| $Bi_2S_3$ | Orthorhombic ($Pbnm$) | 6 | 88.30 | 2.06 | [15], [13] |
| $Bi_2Se_3$ | Rhombohedral ($R\bar{3}m$) | 6 | 86.50 | 2.4 | [14], [13] |
| $Bi_2Te_3$ | Rhombohedral ($R\bar{3}m$) | 6 | 88.65 | 1.7 | [14], [13] |
| $NaSbS_2$ | Triclinic ($P\bar{1}$) | 4 | 92.00 | 2.22 | [9], [16] |
| $KSbS_2$ | Monoclinic ($C2/c$) | 4 | 92.80 | 1.58 | [9], [17] |
| $KSbSe_2$ | Triclinic ($P\bar{1}$) | 4 | 93.05 | 1.3 | [9], [16] |
| $RbSbS_2$ | Triclinic ($P\bar{1}$) | 4 | 91.83 | 1.6 | [18], [16] |
| $CsSbS_2$ | Monoclinic ($P21/c$) | 3 | 95.02 | 1.2 | [19], [16] |
| $CuAsSe_2$ | Rhombohedral ($R3m$) | 4 | 107.82 | 3.2 | [20], [13] |
| $CuSbS_2$ | Orthorhombic ($Pnma$) | 3 | 95.84 | 1.5 | [6], [13] |
| $CuSbSe_2$ | Orthorhombic ($Pnma$) | 3 | 95.24 | 1.49 | [6], [a] |
| $CuBiS_2$ | Orthorhombic ($Pnma$) | 5 | 96.13 | 0.5 | [21], [13] |
| $AgSbS_2$ | Monoclinic ($C121$) | 5 | 94.85 | 0.49 | [22], [13] |
| $AgSbS_2$ | Cubic ($Fm3m$) | 6 | 90.00 | 0.402 | [23], [a] |
| $AgSbSe_2$ | Cubic ($Fm3m$) | 6 | 90.0 | 0.77 | [24], [13] |
| $AgSbTe_2$ | Cubic ($Fm3m$) | 6 | 90.00 | 0.68 | [24], [5] |
| $AgBiSe_2$ | Cubic ($Fm3m$) | 6 | 90.00 | 0.62 | [24], [5] |
| $TlAsS_2$ | Monoclinic ($P21/a$) | 3 | 99.17 | 0.95 | [25], [17] |
| $TlSbS_2$ | Triclinic ($P1$) | 4 | 93.50 | 1.2 | [9], [17] |
| $TlBiS_2$ | Rhombohedral ($R\bar{3}m$) | 6 | 90.00 | 0.875 | [26], [17] |
| $Cu_3AsS_3$ | Orthorhombic ($Pnma$) | 3 | 98.37 | 1.1 | [22], [13] |
| $Cu_3SbSe_3$ | Orthorhombic ($Pnma$) | 3 | 99.42 | 0.49 | [8], [a] |
| $Tl_3SbS_3$ | Rhombohedral ($R3m$) | 3 | 99.20 | 0.42 | [27], [13] |
| $K_2Bi_8Se_{13}$ | Triclinic ($P\bar{1}$) | 6 | 86.83 | 3.1 | [19], [28] |
| $\beta$-$K_2Bi_8Se_{13}$ | Monoclinic ($P21/m$) | 6 | 89.05 | 1.28 | [28] |
| $AgBi_3S_5$ | Monoclinic ($C2/m$) | 6 | 89.08 | 1.2 | [29] |
| $Cu_3AsS_4$ | Orthorhombic ($Pmn21$) | 4 | 109.50 | 3.02 | [30] |
| $Cu_3SbS_4$ | Tetragonal ($I\bar{4}2m$) | 4 | 109.50 | 2.7 | [30], [13] |
| $Cu_3AsSe_4$ | Cubic ($Pm3m$) | 4 | 109.50 | 2.7 | [30] |
| $Cu_3SbSe_4$ | Tetragonal ($I\bar{4}2m$) | 4 | 109.50 | 2.9 | [7], [a] |

[a] Indicates that $\kappa_L$ was measured as a part of this work. Refer to the Supplemental Material [11] for details regarding sample synthesis and characterization.

The room temperature $\kappa_L$ versus average $X$-$M$-$X$ bond angle ($\bar{\alpha}$) of the compounds listed in Table I and plotted in Fig. 3 corroborate the trend observed in the Cu-Sb-Se system. The broad minimum in $\kappa_L$ lies intermediate to the smallest ($\bar{\alpha} = 86.5°$) and largest ($\bar{\alpha} = 109.5°$) $\bar{\alpha}$ values, where the LEP is far removed from the nucleus of the $M$ atom without forming an $M$-$X$ bond. Several of the compounds with intermediate $\bar{\alpha}$ have $\kappa_L$ in the range of the estimated $\kappa_{\min}$ values for these compounds (indicated by the shaded region in Fig. 3) (Refer to the Supplemental Material [11] for more detail regarding $\kappa_{\min}$ calculations).

Although the general trend of decreasing $\kappa_L$ with increasing $\bar{\alpha}$ (for $\bar{\alpha} < 100°$) is clearly illustrated in Fig. 3 there is considerable scatter in the data, particularly for the intermediate ($\bar{\alpha} = 90$–$100°$) bond angles. To better understand the influence of LEPs on $\kappa_L$ we must look closer at the local atomic environment of the $M$ atom. Figure 4 shows the data from Fig. 3 (excluding the compounds with $\bar{\alpha}$ near 109.5° since they do not contain LEPs, as discussed above) plotted separately according to the coordination number (CN) of the $M$ atom, which corresponds to the number of nearest neighbor chalcogen atoms surrounding the $M$ atom. For each CN group, $\kappa_L$ decreases nearly linearly with increasing $\bar{\alpha}$, suggesting that $\kappa_L$ depends on not only the morphology of the LEP, but also the nature of the $MX_n$ polyhedra.

Figure 4 also shows that $\kappa_L$ decreases more rapidly with increasing CN, as indicated by the changing slope of the line of best fit (dashed lines in Fig. 4). For compounds with $\mathrm{CN} \geq 6$ (octahedral or greater coordination) the slope is $-0.64$, while for $\mathrm{CN} = 4$–$5$ (trigonal bypyramidal-like coordination) and $\mathrm{CN} = 3$ (trigonal pyramidal

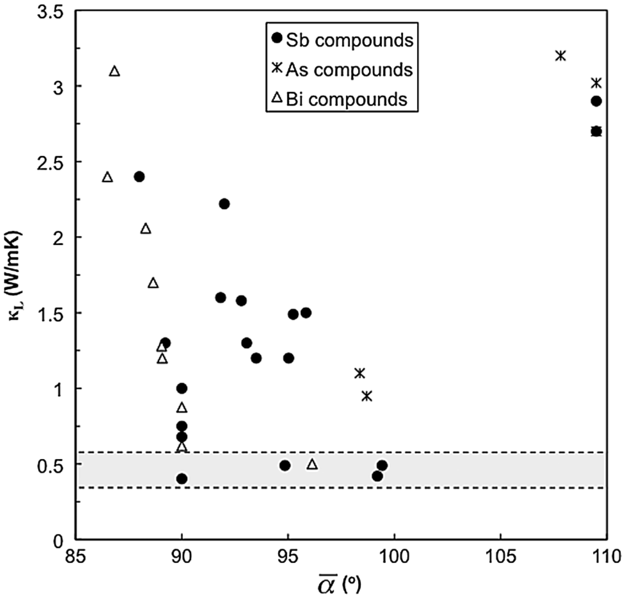

FIG. 3. Room temperature lattice thermal conductivity ($\kappa_L$) versus average $X$-$M$-$X$ bond angle ($\bar{\alpha}$) for binary and ternary group VA chalcogenides of the form $M_2X_3$ and $A_iM_jX_k$ where $M$ = As, Sb, or Bi, $X$ = S, Se, or Te, and $A$ = Cu, Ag, Tl, or an alkali metal (see Table I for a complete list of compounds). Shaded region indicates the range of estimated $\kappa_{\min}$ values for the compounds in Table I.

coordination) it is −0.37 and −0.18, respectively. When the $M$ atom has CN ≥ 6, atomic packing rules require that is it surrounded by chalcogen atoms on all sides. In this case the LEP assumes a spherical distribution around the $M$ nucleus, and any small retraction of the LEP away from the nucleus will cause a strong repulsion with a nearby negatively charged chalcogen atom (see Supplemental Material [11] for supporting arguments). The maximum $X$-$M$-$X$ bond angle for CN = 6 is 90° (NaCl-type structure), and all of the compounds that fall into this category have $\kappa_L < 1.0$ W/mK at room temperature.

The $M$ atoms in compounds with CN = 4–5 have essentially octahedral coordination with 2 or 3 of the chalcogen atoms far removed from their ideal octahedral positions. In this arrangement, the LEP is retracted from the $M$ nucleus in the direction of the missing chalcogen atom(s). The absence of a complete octahedron around the $M$ atom results in a more gradual decrease of $\kappa_L$ with $\bar{\alpha}$ due to less interaction between the LEP and surrounding chalcogen atoms. For CN = 3 the $M$ atom is surrounded by exactly 3 chalcogen atoms in a trigonal pyramid and the LEP is retracted from the nucleus towards the missing link of the tetrahedron. The absence of nearby chalcogen atoms in this direction means that strong lattice anharmonicity will not be achieved until the LEP is far removed from the $M$ nucleus, and indeed low $\kappa_L$ values are not observed in these compounds until $\bar{\alpha} > 98$–$100°$. Similar compounds with CN = 3 and $\bar{\alpha} > 100°$ are rare but have exceedingly low $\kappa_L$, for example $\mathrm{Tl_3AsSe_3}$ which has $\bar{\alpha} = 118°$ and $\kappa_L = 0.35$ W/m*K at room temperature [31,32].

We have demonstrated that the interaction of lone-pair electrons with neighboring atoms can produce minimum lattice thermal conductivity in group VA chalcogenide compounds. Both the morphology of the lone-pair electron orbital and the coordination environment of the group VA atom affect the extent to which the LEPs induce anharmonicity in the crystal lattice. Based on these results, the propensity of a given group VA chalcogenide compound to exhibit $\kappa_{\min}$ behavior can be evaluated based solely on crystallographic data. For compounds with CN ≥ 6, $X$-$M$-$X$ bond angles close to $\bar{\alpha} = 90°$ are preferred, whereas for CN = 4–5 and 3 $\bar{\alpha}$ should be 95–96° and >99°, respectively, to achieve $\kappa_{\min}$ behavior. These guidelines could prove useful in identifying potential new compounds for thermoelectric applications as well as thermal barrier coatings.

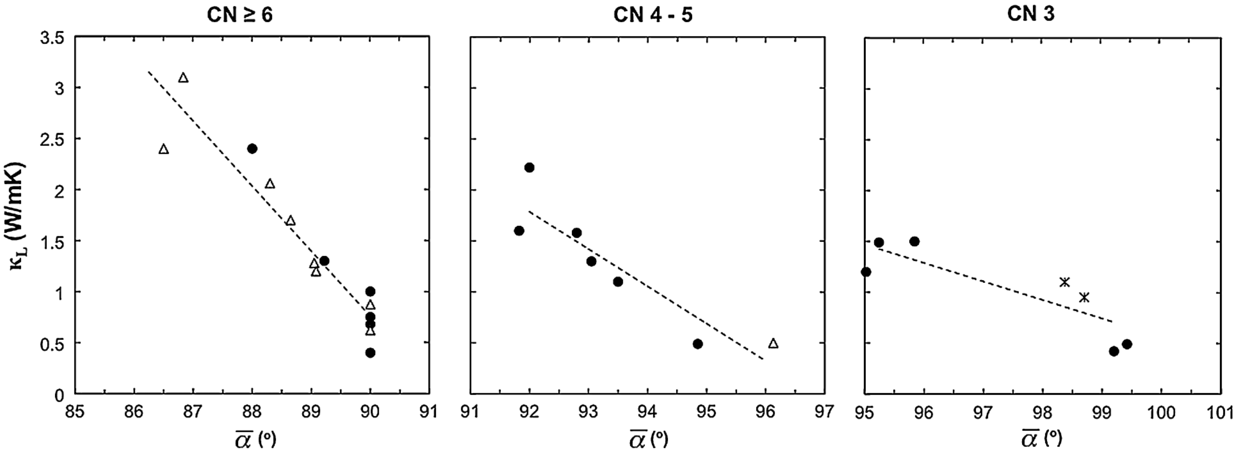

FIG. 4. Data from Fig. 3 plotted in three separate groups according to coordination number of the group VA atom. Dashed lines indicate linear approximations to the data.

We thank Paul Majsztrik, Melanie Kirkham, and Edgar Lara-Curzio for helping to refine the synthesis procedure of the Cu-Sb-Se compounds; Jeffrey D. Cain for assisting in synthesis and characterization; and Dat Do, S. D. Mahanti, Yongsheng Zhang, and Chris Wolverton for providing theoretical insight. This work is supported by the National Science Foundation under Award No. NSF-CBET-0754029. In addition, sample synthesis efforts were partially supported as part of the Center for Revolutionary Materials for Solid State Energy Conversion, an Energy Frontier Research Center funded by the U.S. Department of Energy, Office of Science, Office of Basic Energy Sciences under Award No. DE-SC0001054.

---

*Corresponding author.

[1] P. Debye, Ann. Phys. (Leipzig) **344**, 789 (1912).
[2] G. A. Slack, Solid State Phys. **34**, 1 (1979).
[3] E. J. Skoug, J. D. Cain, and D. T. Morelli, Appl. Phys. Lett. **96**, 181905 (2010).
[4] A. V. Petrov and E. L. Shtrum, Sov. Phys. Solid State **4**, 1061 (1962).
[5] D. T. Morelli, V. Jovovic, and J. P. Heremans, Phys. Rev. Lett. **101**, 035901 (2008).
[6] J. Zhou *et al.*, J. Solid State Chem. **182**, 259 (2009).
[7] A. Pfitzner, Z. Kristallogr. **209**, 685 (1994).
[8] A. Pfitzner, Z. Anorg. Allg. Chem. **621**, 685 (1995).
[9] X. Wang and F. Liebau, Acta Crystallogr. Sect. B **52**, 7 (1996).
[10] Y. Zhang, E. Skoug, J. Cain, C. Wolverton, and D. Morelli (to be published).
[11] See Supplemental Material at http://link.aps.org/supplemental/10.1103/PhysRevLett.107.235901 for a description of the synthesis and characterization methods used in this work along with a brief supplementary discussion section.
[12] A. Kyono, M. Kimata, M. Matsuhisa, Y. Miyashita, and K. Okamoto, Physics and Chemistry of Materials Treatment **29**, 254 (2002).
[13] D. P. Spitzer, J. Phys. Chem. Solids **31**, 19 (1970).
[14] *Antimony Telluride (*Sb2Te3*) Crystal Structure, Chemical Bond, Lattice Parameters (Including Data for* Bi2Se3, Bi2Te3*)* edited by O. Madelung, U. Rössler, and M. Schulz, The Landolt-Börnstein Database Vol. III/17E-17F-41C (SpringerMaterials, Berlin, 1998).
[15] Y. Takéuchi and T. Ozawa, Z. Kristallogr. **141**, 217 (1975).
[16] V. A. Bazakutsa and M. P. Vasil'eva, J. Eng. Phys. Thermophys. **34**, 137 (1978).
[17] V. A. Bazakutsa, M. P. Vasil'eva, V. N. Ustimenko, and L. M. Mokhir, J. Eng. Phys. Thermophys. **37**, 1191 (1979).
[18] A. S. Kanishcheva, V. G. Kuznetsov, V. B. Lazarev, and T. G. Tarasova, J. Struct. Chem. **18**, 849 (1978).
[19] T. J. McCarthy *et al.*, Chem. Mater. **5**, 331 (1993).
[20] K. S. Liang, A. Bienenstock, and C. W. Bates, Phys. Rev. B **10**, 1528 (1974).
[21] J. C. Portheine and W. Nowacki, Z. Kristallogr. **141**, 387 (1975).
[22] Y. Takéuchi and R. Sadanaga, Z. Kristallogr. **130**, 346 (1969).
[23] A. Orliukas, V. Valiukenas, A. Kybartas Kezionis, and V. Vilnius, Ferroelectrics **38**, 897 (1981).
[24] V. P. Zhuze, V. M. Sergeeva, and E. L. Shtrum, Sov. Phys. Tech. Phys. **3**, 1925 (1958).
[25] Z. M. Yang and F. Pertlik, J. Alloys Compd. **216**, 155 (1994).
[26] C. L. Teske and W. Bensch, Acta Crystallogr. Sect. E **62**, i163 (2006).
[27] A. Olsen, P. Goodman, and H. J. Whitfield, J. Solid State Chem. **60**, 305 (1985).
[28] D. Y. Chung *et al.*, Chem. Mater. **9**, 3060 (1997).
[29] J. H. Kim *et al.*, Chem. Mater. **17**, 3606 (2005).
[30] L. I. Berger and V. D. Prochukhan, *Ternary Diamond-Like Semiconductors* (Consultants Bureau, New York, 1969).
[31] H. Y-P. Hong, J. C. Mikkelsen, and G. W. Roland, Mater. Res. Bull. **9**, 365 (1974).
[32] M. D. Ewbank, P. R. Newman, and H. Kuwamoto, J. Appl. Phys. **53**, 6450 (1982).